Coupled-State Calculations of Proton-Hydrogen Scattering in the Sturmian Representation*†

D. F. GALLAHER‡ AND L. WILETS
University of Washington, Seattle, Washington 98105
(Received 13 October 1967)

Proton-hydrogen scattering has been solved in the Sturmian representation. The Sturmian functions of Rotenberg form an infinite, discrete, and complete basis set without a continuum. Comparison has been made with the following proton-hydrogen scattering experiments: transfer and excitation cross sections to the $2s$ and $2p$ states, the total exchange cross section, and the notable experiments of Helbig and Everhart on the total transfer probability at 3°. Particularly excellent agreement is found with the last. This work is a direct extension of previous calculations for the proton-hydrogen scattering problem developed by the authors in which the expansion basis functions were discrete, traveling hydrogenic states. The present work demonstrates the role of the hydrogenic continuum.

I. INTRODUCTION

THE proton-hydrogen atom collision is one of the simplest and most instructive scattering problems available. Although in its full complexity it is a quantum-mechanical three-body problem, the very small electron-proton mass ratio allows one to use the well-known semiclassical impact-parameter formulation where the protons follow a linear classical trajectory and the Schrödinger equation for the three-particle system reduces to a one-electron, time-dependent equation. This impact-parameter approach has been often used and has been shown[1–3] to be valid above a few hundred electron volts incident energy.

In this investigation we follow essentially our previous treatment[4] (hereafter referred to as WG), in which the time-dependent, nonrelativistic, spinless Schrödinger equation is solved numerically. The basis set for the expansion is chosen to be composed of traveling Sturmian functions, a set of functions brought into prominence by Rotenberg[5] is a related problem. The properties of these functions will be described subsequently in greater detail, but their usefulness arises since they form a complete, discrete set without a continuum. This allows us to assess the effect of the continuum on the scattering cross sections and polarizations, which, as will be seen, is quite significant.

We proceed essentially as in WG, making a two-centered expansion in traveling Sturmian orbitals, and utilizing symmetries to reduce the coupled equations. Finally, the physical amplitudes will be obtained from the Sturmian amplitudes by projection.

The ensuing sections deal with the following topics: the Sturmian basis set, use of molecular symmetries, deduction of the coupled equations, projection to obtain the physical scattering amplitudes, convergence, numerical solution of the coupled equations (including matrix-element calculation and time integration), a comparison of results with experiment, and discussion of possible extensions of the problem.

II. STURMIAN BASIS SET

In the impact-parameter approximation we let the distance from proton A (target) to proton B (projectile) be given by

$$\mathbf{R}=\mathbf{b}+\mathbf{v}t. \tag{1}$$

The electron position vector relative to protons A or B is given by

$$\mathbf{r}_{A,B}=\mathbf{r}\pm\tfrac{1}{2}\mathbf{R}, \tag{2}$$

where $\mathbf{r}$ is the electron position vector in the c.m. of the two protons.

We expand the electronic wave function in terms of traveling Sturmian waves about each proton with the Sturmian functions quantized about the interproton axis. The primed rotating coordinate system is such that the z' axis passes through protons A and B. The coordinate system is shown in Fig. 1.

These basis states are then given by

$$w_k\binom{A}{B}=\hat{\phi}_k(\mathbf{r}_{A,B}')e^{\mp ivz/2}\exp[-i(\hat{\epsilon}_k+\tfrac{1}{8}v^2)t] \tag{3}$$

(k stands for the quantum-number set nlm), where

$$\hat{\phi}_k(\mathbf{r}_i')=[S_{nl}(r_i')/r_i']\mathcal{Y}_{lm}(\vartheta_i',\varphi_i'), \tag{4}$$

and the Sturmian functions $S_k(r)=S_{nl}(r)$ satisfy the equation (we use atomic units throughout)

$$\left(-\frac{1}{2}\frac{d^2}{dr^2}+\frac{l(l+1)}{2r^2}-\frac{\alpha_k}{r}\right)S_k(r)=E_lS_k(r). \tag{5}$$

* Supported in part by the U. S. Atomic Energy Commission under Contract No. AT(45-1)1388B.
† Based in part on a Ph.D. thesis submitted to the University of Washington by D.F.G.
‡ Present address: Queen's University of Belfast, Ireland.
[1] M. Mittleman, Phys. Rev. **122**, 499 (1961).
[2] J. W. R. Fennema, thesis, University of Amsterdam, 1967 (unpublished).
[3] L. Wilets and S. J. Wallace, in *Proceedings of the Fifth International Conference on the Physics of Electronic and Atomic Collisions, Leningrad* (Nauka, 1967), p. 62.
[4] L. Wilets and D. F. Gallaher, Phys. Rev. **147**, 13 (1966); D. R. Bates and R. McCarroll, Proc. Roy. Soc. (London) **A245**, 175 (1958); D. R. Bates, *ibid.* **A245**, 299 (1958); D. R. Bates and Griffing, *ibid.* **A66**, 961 (1953); **A67**, 663 (1954); S. E. Lovell and M. B. McElroy, *ibid.* **A283**, 100 (1965).
[5] M. Rotenberg, Ann. Phys. (N. Y.) **19**, 262 (1962).

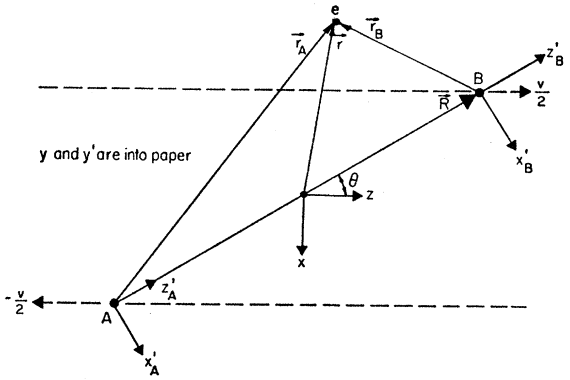

FIG. 1. Representation of the coordinate systems. Unprimed coordinates are measured in the c.m. inertial system. The primed coordinate system rotates with the internuclear axis.

These Sturmian functions $S_k(r)$ were introduced by Rotenberg,[5] who chose $E_l=-\frac{1}{2}$, the ground-state energy of the hydrogen atom. We choose $E_l=-1/[2(l+1)^2]$.

The Sturmian equation is similar to the Schrödinger equation, but the energy E_l appears as a fixed parameter; it is the effective charge α_k which acts as the eigenvalue. The required boundary conditions on $S_k(r)$ are that it be zero at the origin and decay at infinity.

The $\hat{\phi}_k(\mathbf{r})$ form an infinite, discrete and complete set of states. Unlike the hydrogenic functions, there is no continuum.

Our Sturmian functions are explicitly given by scaled hydrogenic functions as

$$S_k(r)=\alpha_k{}^{1/2}R_k(\alpha_k r)\,, \tag{6}$$

where $R_k(r)$ is the usual radial hydrogenic function. The normalization is chosen such that

$$\langle\hat{k}\,|\,\hat{k}\rangle=1\,, \tag{7}$$

$(\hat{\phi}_k\leftrightarrow|\,\hat{k}\rangle)$, but there are nonvanishing matrix elements of $\langle\hat{k}\,|\,\hat{k}'\rangle$ for $k\neq k'$. Cross multiplication and subtraction of the Sturmian equations for k and k' leads to the modified orthogonality condition

$$\langle\hat{k}\,|\,r^{-1}\,|\,\hat{k}'\rangle=(\alpha_k'/n^2)\delta_{kk'}\,. \tag{8}$$

Thus the Sturmian functions are orthogonal with the potential energy r^{-1} as a weighting function.

Since the energy parameter is chosen to be

$$E_l=-1/[2(l+1)^2]\,, \tag{9}$$

manipulation of the Sturmian equation (making the transformation $x=\alpha_k r$) yields

$$\alpha_k=n/(l+1)\,. \tag{10}$$

The mean energy $\hat{\epsilon}_k=\langle\hat{k}\,|\,H\,|\,\hat{k}\rangle$, with $H=-\frac{1}{2}\nabla^2-r^{-1}$, is given by

$$\hat{\epsilon}_k=-1/[n(l+1)]+1/[2(l+1)^2]\,. \tag{11}$$

By the way in which our Sturmian basis set is defined, the $1s$, $2p$, $3d$, etc., Sturmian functions coincide with the corresponding hydrogenic wave functions ϕ_k. In Rotenberg's Sturmian set, only the $1s$ Sturmian function coincides with the $1s$ hydrogenic function. The Sturmian states are more compact than hydrogenic states. This can be seen by noting that

$$\langle\hat{k}\,|\,r^{-1}\,|\,\hat{k}\rangle=1/n(l+1)$$

as compared with

$$\langle k\,|\,r^{-1}\,|\,k\rangle=n^{-2}.$$

As in our previous work, to test the utility of our basis set we calculate the overlap probability with the united atom He^+ ground state. This time the overlap with the first three Sturmian s states gives 0.92, as compared with 0.76 for the overlap with all discrete hydrogenic functions. Inasmuch as the $1s$ He^+ state gives zero overlap with the $2s$ Sturmian state, this is quite remarkable convergence, demonstrating the power of the Sturmian basis to include the hydrogenic continuum.

III. USE OF MOLECULAR SYMMETRIES

Precisely as was done in WG, we make use of the invariance of the Hamiltonian

$$H=-\tfrac{1}{2}\nabla^2-r_A{}^{-1}-r_B{}^{-1}+R^{-1} \tag{12}$$

under reflection through the collision plane ($\varphi'\rightarrow-\varphi'$) and inversion through the c.m. of the two protons ($\mathbf{r}\rightarrow-\mathbf{r}$ and $\mathbf{r}_{A,B}\rightarrow-\mathbf{r}_{B,A}$).

We utilize first the azimuthal symmetry, which assures that the wave function satisfies the relation

$$\Psi(r,\vartheta',\varphi',t)=\Psi(r,\vartheta',-\varphi',t) \tag{13}$$

for all times, since it is satisfied initially. This allows us to consider only positive m values (m is the magnetic quantum number) by defining the spherical harmonics as

$$\mathcal{Y}_{lm}(\vartheta',\varphi')=\begin{cases}Y_{l0}, & m=0\\ 2^{-1/2}[Y_{lm}+(-)^mY_{l-m}], & m>0.\end{cases} \tag{14}$$

The second invariance of H under $\mathbf{r}\rightarrow-\mathbf{r}$ assures parity conservation. As before, we choose a Sturmian basis set combined from $w_k(A)$ and $w_k(B)$ as

$$W_k{}^{\pi}(\mathbf{r},t)=2^{-1/2}[w_k(A)+\pi(-1)^lw_k(B)]\,, \tag{15}$$

where the parity operator Π transforms w_k according to

$$\Pi w_k\begin{pmatrix}A\\B\end{pmatrix}=(-1)^lw_k\begin{pmatrix}B\\A\end{pmatrix}. \tag{16}$$

We again decompose the total wave function Ψ into parity wave functions as

$$\Psi=2^{-1/2}[\Psi^+\!+\Psi^-]\,, \tag{17}$$

where

$$\Psi^{\pi}=\sum_k b_k{}^{\pi}(t)W_k{}^{\pi}(\mathbf{r},t), \tag{18}$$

so that we have

$$\Psi(\mathbf{r},t)=\tfrac{1}{2}\sum_k\{(b_k{}^{+}+b_k{}^{-})w_k(A) +(-1)^l(b_k{}^{+}-b_k{}^{-})w_k(B)\}. \tag{19}$$

To facilitate the projection of the Sturmian basis set onto the hydrogenic physical basis set, we reiterate here from WG the corresponding expansions in the hydrogenic basis:

$$U_k{}^{\pi}(\mathbf{r},t)=2^{-1/2}[u_k(A)+\pi(-1)^l u_k(B)], \tag{20}$$

where

$$u_k\binom{A}{B}=\phi_k(\mathbf{r}_{A,B})e^{\mp ivz/2}e^{-i(\epsilon_k+v^2/8)t} \tag{21}$$

and

$$\phi_k(\mathbf{r}')=r^{-1}R_{nl}(r)\mathcal{Y}_{lm}(\vartheta',\varphi'). \tag{22}$$

There we expanded Ψ^{π} as $\Psi^{\pi}=\sum_k a_k{}^{\pi}(t)U_k{}^{\pi}(\mathbf{r},t)$, so that

$$\Psi=\tfrac{1}{2}\sum_k\{a_k{}^{+}+a_k{}^{-})u_k(A) +(-1)^l(a_k{}^{+}-a_k{}^{-})u_k(B)\}, \tag{23}$$

in which the $a_k{}^{\pi}(t)$ are "physical" time-dependent amplitudes. The initial condition of the electron on the target proton in the ground state reduces to the condition

$$a_k{}^{\pi}(-\infty)=b_k{}^{\pi}(-\infty)=\delta_{1,k}, \tag{24}$$

since the $1s$ Sturmian state corresponds to the $1s$ hydrogenic state.

Hence the hydrogenic amplitudes for direct and exchange reactions are the asymptotic values of the coefficients of $u_k(A)$ and $u_k(B)$, namely,

$$a_k{}^{d,x}=\tfrac{1}{2}[a_k{}^{+}(\infty)\pm a_k{}^{-}(\infty)]. \tag{25}$$

These amplitudes $a_k{}^{d,x}$ will be obtained in terms of the Sturmian amplitudes by projection (Sec. V).

IV. COUPLED EQUATIONS

We wish to solve the time-dependent Schrödinger equation

$$i\dot{\Psi}=H\Psi, \tag{26}$$

with H given by Eq. (12). Since we are dealing with a truncated basis set, this cannot be done exactly, but rather we minimize the variational function

$$\int_{-\infty}^{\infty}dt\int d\mathbf{r}\Psi^{*}(H-i\partial/\partial t)\Psi. \tag{27}$$

With the expansion (18), this leads to the coupled equations (compare WG)

$$i\sum_{k'}N_{kk'}{}^{\pi}\dot{b}_{k'}{}^{\pi}=\sum_{k'}H_{kk'}{}^{\pi}b_{k'}{}^{\pi}, \tag{28}$$

where

$$N_{kk'}{}^{\pi}=\int d\mathbf{r}\,W_k{}^{\pi *}W_{k'}{}^{\pi}=[\langle\hat{k}|\hat{k}'\rangle+\pi(-)^l\langle\hat{k}B|e^{-ivz}|\hat{k}'A\rangle]\exp[i(\hat{\epsilon}_n-\hat{\epsilon}_{n'})t]\equiv\hat{N}_{kk'}{}^{\pi}\exp[i(\hat{\epsilon}_n-\hat{\epsilon}_{n'})t], \tag{29}$$

$$\begin{aligned}H_{kk'}{}^{\pi}=\int d\mathbf{r}\,W_k{}^{\pi *}(H-i\partial/\partial t)W_{k'}{}^{\pi}=\Bigg\{&\frac{\hat{N}_{kk'}{}^{\pi}}{R}-\left\langle\hat{k}A\left|\frac{1}{r_B}\right|\hat{k}'A\right\rangle+\left[\frac{1}{n'(l'+1)}-\frac{1}{(l'+1)^2}\right][\hat{N}_{kk'}{}^{\pi}-\delta_{kk'}]\\&+\pi(-)^l\left[\left(\frac{n'}{l'+1}-1\right)\left\langle\hat{k}B\left|\frac{e^{-ivz}}{r_A}\right|\hat{k}'A\right\rangle-\left\langle\hat{k}B\left|\frac{e^{-ivz}}{r_B}\right|\hat{k}'A\right\rangle\right]\\&+(d\Theta/dt)[\langle\hat{k}A|l_A|\hat{k}'A\rangle+\pi(-)^l\langle\hat{k}B|e^{-ivz}l_A|\hat{k}'A\rangle]\Bigg\}\exp[i(\hat{\epsilon}_n-\hat{\epsilon}_{n'})t]\equiv\hat{H}_{kk'}{}^{\pi}\exp[i(\hat{\epsilon}_n-\hat{\epsilon}_{n'})t],\end{aligned} \tag{30}$$

in the notation

$$|\hat{k}A\rangle\leftrightarrow\hat{\phi}_k(\mathbf{r}_A'),$$

$$l_A\equiv(l_{y'})_A=-i\left(z_{A'}\frac{\partial}{\partial x_{A'}}-x_{A'}\frac{\partial}{\partial z_{A'}}\right),$$

$$\Theta=\tan^{-1}(b/vt).$$

In the matrix notation, we have

$$i\mathbf{N}\dot{\mathbf{b}}=\mathbf{H}\mathbf{b} \tag{31}$$

or

$$i\dot{\mathbf{b}}=\mathbf{N}^{-1}\mathbf{H}\mathbf{b}=\mathbf{G}\mathbf{b}. \tag{32}$$

V. ASYMPTOTIC AMPLITUDES

Because the Sturmian states are not solutions of the hydrogen problem, and because the set is truncated, the projected hydrogenic amplitudes $a_k(t)$ contain frequency components other than $\exp[-i(\hat{\epsilon}_k+\frac{1}{8}v^2)t]$. The corresponding probabilities $|a_k(t)|^2$ thus contain oscillatory components for large time, in addition to the expected secular part. The presence of the oscillatory component is one measure of the failure of the expansion (and is small for the low hydrogenic states). In computing probabilities, we remove the oscillatory com-

ponents explicitly. To see how this is done, let us consider the time integration to have been carried to a point $t=t_m$ such that only asymptotic coupling remains. The superscripts π, direct, or exchange, will be suppressed, since the matrix elements are asymptotically identical.

Let

$$\beta_k(t)=b_k(t)\exp(-i\hat{\epsilon}_k t); \tag{33}$$

then

$$i\dot{\beta}=\mathbf{U}\beta, \tag{34}$$

where

$$U_{kk'}=\hat{G}_{kk'}+\hat{\epsilon}_{k'}\delta_{kk'} \tag{35}$$

is time-independent. Let $\mathbf{T}$ be a time-independent matrix which diagonalizes $\mathbf{U}$:

$$\mathbf{TUT}^{-1}=\mathbf{W} \tag{36}$$

and

$$\gamma\equiv\mathbf{T}\beta. \tag{37}$$

The γ satisfy

$$i\dot{\gamma}=\mathbf{W}\gamma \tag{38}$$

or

$$\gamma_k=\gamma_k(t_m)e^{-iw_k(t-t_m)},\quad t\gtrsim t_m. \tag{39}$$

This yields

$$a_k(t)=e^{-i\epsilon_k t}\sum_{k'k''k'''}\langle k|\hat{k}'\rangle(T^{-1})_{k'k''}\times\exp[-iw_{k''}(t-t_m)]T_{k''k'''}\beta_{k'''}(t_m). \tag{40}$$

The probabilities are given by

$$P_k=|a_k(t)|^2=\sum_{k''}|C_{kk''}|^2+(\text{oscillating term}), \tag{41}$$

where

$$C_{kk''}=\sum_{k'k'''}\langle k|\hat{k}'\rangle(T^{-1})_{k'k''}T_{k''k'''}\beta_{k'''}(t_m). \tag{42}$$

The asymptotic form of $\mathbf{U}$ is given by

$$U_{kk'}=(N^{-1})_{kk''}(\hat{\epsilon}_{k'}+E_{l'})(N_{k''k'}-\delta_{k''k'})+\hat{\epsilon}_k\delta_{kk'}, \tag{43}$$

where $N_{k''k'}\rightarrow\langle\hat{k}''|\hat{k}'\rangle$ is given in Sec. VI. Explicit formulas for calculating the P_k are given in Table I.

Total exchange probabilities are handled somewhat differently in the Sturmian expansion than was the case in the hydrogenic expansion, since the Sturmian states include the continuum and hence ionization states. As before, our normalization condition is

$$\int d\mathbf{r}\,|\Psi|^2=\sum_{kk'}b_k^*(t)N_{kk'}b_{k'}(t)=1, \tag{44}$$

compared with the result $\sum|a_k|^2=1$ in the hydrogenic case. We again may differentiate this condition with respect to time to obtain the useful matrix equation

$$i\mathbf{dN}/dt+\mathbf{H}-\mathbf{H}^\dagger=\mathbf{0} \tag{45}$$

as an invaluable aid in tracking subtle programming errors. Thus we have the probability summation given by

$$P^{\text{ion}}+\sum(P_k{}^d+P_k{}^x)=1, \tag{46}$$

where the sum is over bound states and p^{ion} is the probability left in the continuum. In general $\sum(P_k{}^d+P_k{}^x)<1$, unlike the hydrogenic case where $\sum(P_k{}^d+P_k{}^x)=1$ since only bound states were included.

In analogy to our hydrogenic calculation (WG), we define pseudodirect and exchange probabilities (including indeterminate ionization) as

$$P_{\text{tot}}{}^{\text{pseudo}-d,x}=\tfrac{1}{4}\sum_{kk'}[b_k{}^{+*}(t_m)\pm b_k{}^{-*}(t_m)]\langle\hat{k}|\hat{k}'\rangle\times[b_{k'}{}^{+}(t_m)\pm b_{k'}{}^{-}(t_m)]\exp[i(\hat{\epsilon}_k-\hat{\epsilon}_{k'})t_m], \tag{47}$$

with

$$P_{\text{tot}}{}^{\text{pseudo}-d}+P_{\text{tot}}{}^{\text{pseudo}-x}=1. \tag{48}$$

We use $P_{\text{tot}}{}^{\text{pseudo}-x}$ to make comparison with the experimental total exchange probabilities (which do not include ionization).

The probability convergence with respect to trajectory length is demonstrated here in Fig. 2, which plots the various probabilities in a four-state $(1s,2s,2p)$ calculation at 25 keV from $Z_m(=t_mv)$ of 10 to $Z_m=30$. One immediately notes that by $Z_m\simeq 20$ the probabilities at 25 keV have converged, while not until $Z_m\simeq 30$ have they converged at 9 keV. Hence the calculations have been carried out to $Z_m=20$ at and above 25 keV, to $Z_m=25$ from 5 to 16 keV inclusive and to $Z_m=30$ below 5 keV.

TABLE I. s-state probabilities in six-state expansion.

$$P_{2s}=|\textstyle\sum_{k'}\langle 2s|\hat{k}'\rangle\beta_{k'}|^2+0.112|\beta_{2s}|^2+0.045|\beta_{3s}|^2-0.130|\beta_{4s}|^2+\mathrm{Re}\{-0.154\beta_{2s}{}^*\beta_{3s}+0.008\beta_{2s}{}^*\beta_{4s}+0.244\beta_{3s}{}^*\beta_{4s}\}$$

$$P_{3s}=|\textstyle\sum_{k'}\langle 3s|\hat{k}'\rangle\beta_{k'}|^2-0.020|\beta_{2s}|^2-0.017|\beta_{3s}|^2+0.029|\beta_{4s}|^2+\mathrm{Re}\{0.078\beta_{2s}{}^*\beta_{3s}+0.044\beta_{2s}{}^*\beta_{4s}-0.092\beta_{3s}{}^*\beta_{4s}\}$$

$$P_{4s}=|\textstyle\sum_{k'}\langle 4s|\hat{k}'\rangle\beta_{k'}|^2+0.065|\beta_{2s}|^2-0.007|\beta_{3s}|^2+0.008|\beta_{4s}|^2+\mathrm{Re}\{0.008\beta_{2s}{}^*\beta_{3s}+0.008\beta_{2s}{}^*\beta_{4s}-0.008\beta_{3s}{}^*\beta_{4s}\}$$

$$\beta^{d,x}=\tfrac{1}{2}[\beta^+(t_m)\pm\beta^-(t_m)]$$

VI. NUMERICAL METHODS

The coupled equations involve the following types of matrix elements:

$$\langle\hat{k}|\hat{k}'\rangle,$$
$$\langle\hat{k}B|e^{-ivz}|\hat{k}'A\rangle,$$
$$\langle\hat{k}B|e^{-ivz}r_{A,B}{}^{-1}|\hat{k}'A\rangle,$$
$$\langle\hat{k}A|r_B{}^{-1}|\hat{k}'A\rangle.$$

We also have the Coriolis matrix elements $\langle\hat{k}B|e^{-ivz}l_A\times|\hat{k}'A\rangle$ and $\langle\hat{k}B|e^{-ivz}r_B{}^{-1}l_A|\hat{k}'A\rangle$, which can be reduced to the above types by operation with l_A on $|\hat{k}'A\rangle$. The

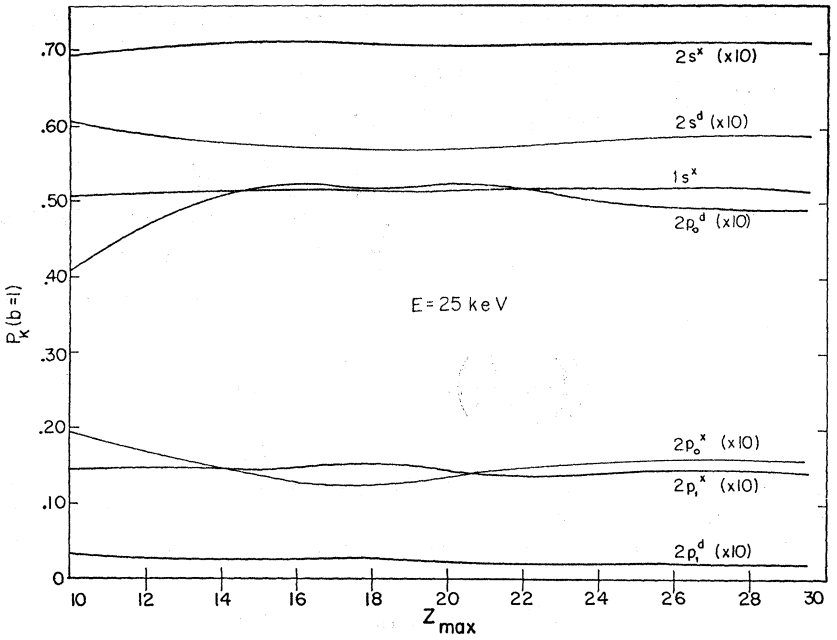

FIG. 2. Dependence of final probabilities on the length ($2Z_m$) of the trajectory: $E=25$ keV, $b=1$, four-state expansion.

projection problem brings in the overlap matrix elements $\langle k|\hat{k}'\rangle$ also. We have the relation

$$\langle \hat{k}B|e^{-ivz}r_B^{-1}|\hat{k}'A\rangle=(-)^{l-l'}\langle \hat{k}'B|e^{-ivz}r_A^{-1}|\hat{k}A\rangle^*, \quad (49)$$

so that there are five independent matrix-element types to be distinguished.

Analytical formulas have been found for the $\langle \hat{k}|\hat{k}'\rangle$ and $\langle k|\hat{k}'\rangle$ elements; the $\langle \hat{k}A|r_B^{-1}|\hat{k}'A\rangle$ may also be integrated in closed form for a given (k,k') pair although a general formula has not been obtained; the e^{-ivz} elements were integrated numerically.

By utilizing the integral formula

$$\int_0^\infty z^p e^{-z} L_{m+p-\mu}^{p-\mu}(z) L_{n+p-\nu}^{p-\nu}(z)\,dz=(-1)^{n+m+\mu+\nu}(2p+m-2\mu)!(2p+n-2\nu)!\mu!\nu!$$
$$\times\sum_\sigma \frac{(p+\sigma)!}{\sigma!(p+m-\mu-\sigma)!(p+m-\nu-\sigma)!(\sigma+2\mu-m-p)!(\sigma+2\nu-n-p)!} \quad (50)$$

(Morse and Feshbach[6]), the $\langle \hat{k}|\hat{k}'\rangle$ elements can be shown to be given by

$$\langle \hat{k}|\hat{k}'\rangle=\frac{1}{2}\left[\frac{(n-l-1)!(n'-l-1)!}{nn'(n+l)!(n'+l)!}\right]^{1/2}(-1)^{n+n'}\sum_\sigma \frac{(2l+\sigma+2)!}{\sigma!(n-l-\sigma-1)!(n'-l-\sigma-1)!(\sigma+2-n+l)!(\sigma+2-n'+l)!}. \quad (51)$$

The cases of s and p states reduce to $(n'\gtrless n)$

$$\langle \hat{n}s|\hat{n}'s\rangle=\delta_{nn'}-\tfrac{1}{2}\delta_{n',n+1}, \quad \langle \hat{n}p|\hat{n}'p\rangle=\delta_{nn'}-\frac{1}{2}\left[1-\frac{2}{n(n+1)}\right]^{1/2}\delta_{n',n+1}, \quad (52)$$

with the interesting property that $\langle \hat{n}p|\hat{n}'p\rangle \xrightarrow[n\to\infty]{} \langle \hat{n}s|\hat{n}'s\rangle$.

By using the generating relation for the Laguerre polynomials

$$(1+t)^a e^{-xt}=\sum_{p=0}^\infty \frac{t^p}{a!}L_a^{a-p}(x)(-1)^{a-p} \quad (53)$$

(Morse and Feshbach[6]), and the binomial expansion, one may, by identifying terms on either side of a power-series

[6] P. M. Morse and H. Feshbach, *Methods of Theoretical Physics, Part I* (McGraw-Hill Book Co., New York, 1953), pp. 784, 785.

expansion, reduce $\langle\hat{k}|\hat{k}'\rangle$ to a complicated double summation formula given by

$$\langle nlm|\hat{n}'l'm\rangle=\left[\frac{(n-l-1)!(n'-l-1)!}{4nn'(n+l)!(n'+l)!}\right]^{1/2}\frac{(2l+2)!}{[n(l+1)]^{l+3/2}}$$
$$\times\sum_{\lambda\mu}\frac{\binom{n+l}{\lambda}\binom{n'+l}{\mu}\binom{-2l-3}{n'+n-2(l+1)-\lambda-\mu}\binom{n'+n-2(l+1)-\lambda-\mu}{n-l-1-\lambda}}{\alpha^{1+n+n'-\lambda-\mu}n^{n-l-1-\lambda}(l+1)^{n'-l-1-\mu}} \quad (54)$$

in which

$$\alpha=\frac{1}{2}\left(\frac{1}{n}+\frac{1}{l+1}\right). \quad (55)$$

To indicate the numerical overlap of $\langle k|$ and $|\hat{k}'\rangle$, these elements are given in Table II. for the sequence of states $1s$, $2s$, $2p$, $3s$, $3p$, $4s$.

By employing the relation for the angular-momentum operators $l^{\pm}$ given by

$$l^{\pm}Y_{lm}=[(l\mp m)(l\pm m+1)]^{\frac{1}{2}}Y_{lm\pm1} \quad (56)$$

(where $l^{\pm}=l_x\pm l_y$) we reduce the Coriolis term $(\alpha\dot{\Theta})$ to

$$-i\dot{\Theta}\left\{\left[\frac{(l-m)(l+m+1)}{2-\delta_{m,0}}\right]^{1/2}N_{k,k'+1}\right.$$
$$\left.-(1-\delta_{m,0})\left[\frac{(l+m)(l-m+1)}{2(2-\delta_{m,0})}\right]^{1/2}N_{k,k'-1}\right\}, \quad (57)$$

in which $k\pm1$ indicates $nlm\pm1$.

The basic matrix elements involving e^{ivz} are evaluated precisely as in WG, using a confocal elliptic coordinate system, transforming e^{ivz} into the rotating reference frame, and calculating numerically the integrals by Gaussian quadrature.

The basic integrals obtained for the three elements given in Eqs. (24) of WG remain the same here with the replacement $|k\rangle\rightarrow|\hat{k}\rangle$.

The same scheme used in WG was again adopted for the time integration of $i\dot{\mathbf{b}}=\mathbf{G}\mathbf{b}$.

VII. FOUR-STATE RESULTS

The great bulk of the calculations have been done coupling the four Sturmian states ($1s$, $2s$, $2p$) in the laboratory energy range from 1 to 1000 keV. The four-

TABLE II. Overlap matrix elements $\langle k|\hat{k}\rangle$.

k \ $\hat{k}$	$1s$	$2s$	$3s$	$4s$	$2p$	$3p$
$1s$	1	−0.5	0	0	0	0
$2s$	0	0.558	−0.870	0.683	0	0
$3s$	0	0.244	−0.244	−0.091	0	0
$4s$	0	0.147	−0.125	−0.103	0	0
$2p$	0	0	0	0	1	−0.409
$3p$	0	0	0	0	0	0.722

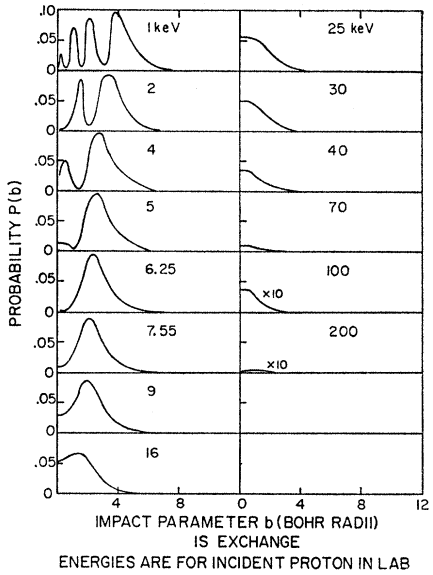

FIG. 3. Probability of excitation versus impact parameter for $1s$ exchange over the energy spectrum from 1 to 1000 keV in the four-state ($1s$,$2s$,$2p$) Sturmian expansion.

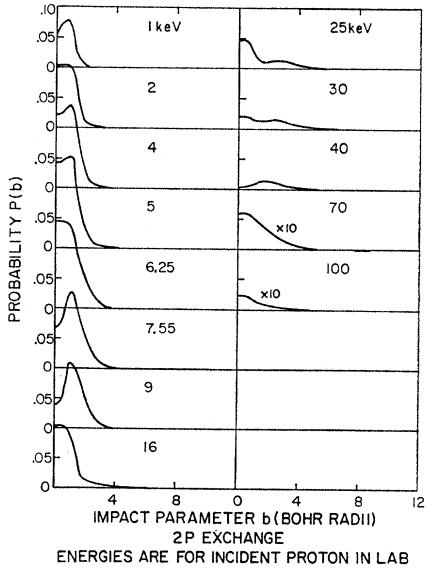

FIG. 4. Probability of excitation versus impact parameter for $2p$ exchange over the energy spectrum from 1 to 1000 keV in the four-state ($1s$,$2s$,$2p$) Sturmian expansion.

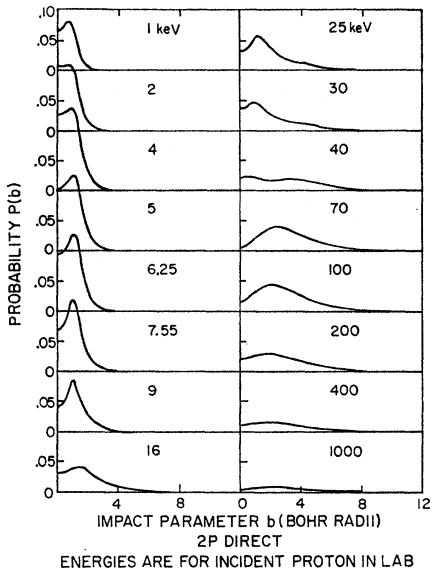

FIG. 5. Probability of excitation versus impact parameter for $2p$ direct excitation over the energy spectrum from 1 to 1000 keV in the four-state ($1s$, $2s$, $2p$) Sturmian expansion.

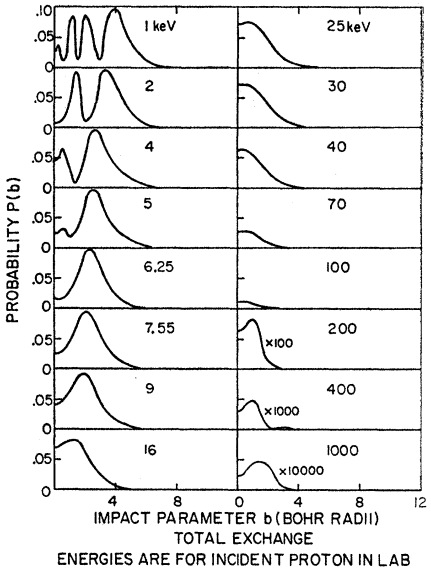

FIG. 6. Probability of excitation versus impact parameter for total exchange over the energy spectrum from 1 to 1000 keV in the four-state ($1s$, $2s$, $2p$) Sturmian expansion.

state results are discussed in this section; higher state results being discussed in Sec. VIII.

Plots of probability versus impact parameter for various energies in the 1–1000 keV range are displayed in Figs. 3–6 for the direct process $2p$, for the exchange processes $1s$, $2p$, and for total exchange. We note that the majority of these curves exhibit a single, well defined peak at from one to two Bohr radii, the peak for the s state processes being generally at smaller b than that for p state processes. This may be explained classically from the relation

$$l = bv \tag{58}$$

(in atomic units) between orbital angular-momentum quantum number l, impact parameter b, and velocity v. The relation shows that for given v, small b is associated with small l and large b with large l (van den Bos[7]).

Note the oscillations in $P(b)$ versus b for $1s$ exchange and total exchange at small impact parameters below

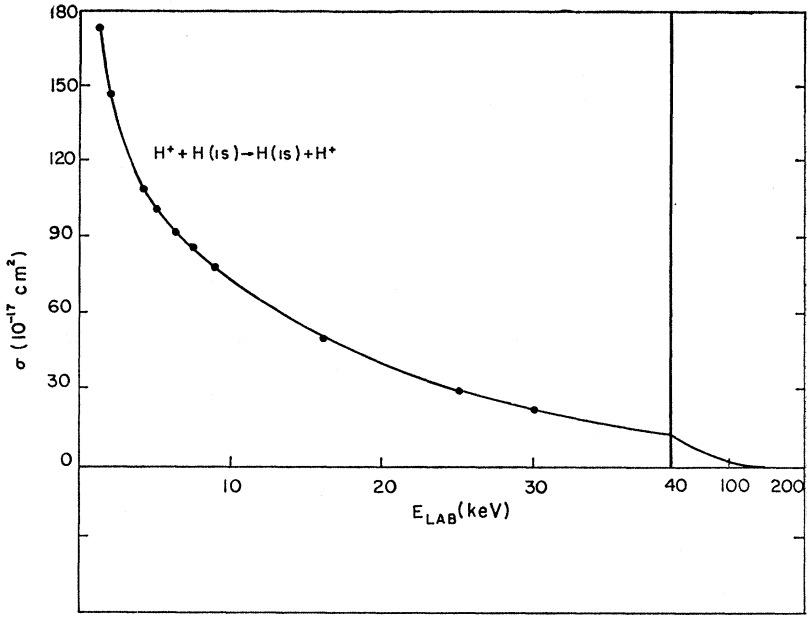

FIG. 7. Ground-state resonant transfer (charge exchange) cross section in the four-state expansion.

[7] J. van den Bos, Foundation for Fundamental Research on Matter (Netherlands) Report No. FOM22358, 1966 (unpublished).

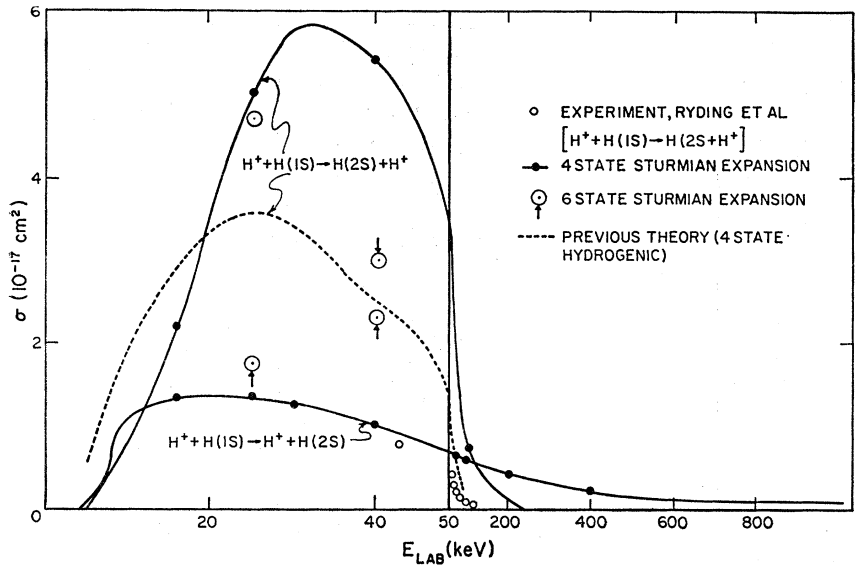

FIG. 8. Cross section for charge transfer and excitation to the $2s$ state in the four-state expansion. The experimental data from 40 to 200 keV are due to Ryding *et al.* (Ref. 8) for charge transfer. These points have been normalized (dubiously) to lie on the theoretical Born-approximation result at 100 keV. The previous theoretical curve for the charge-transfer reaction is that obtained in the four-state hydrogenic expansion. The circles are for a six-state ($1s$,$2s$,$2p$, $3s$,$4s$) Sturmian calculation.

6 keV. This is attributable to multiple exchanges of the electron to the ground state for low energies and small impact parameters. As the energy increases, the direct probabilities dominate the exchange, approaching, at high energies, Rutherford elastic scattering. There is also evidence that the $2p$ probabilities dominate the $2s$ at all energies. This is interpreted as due to the $2p$ being an optically allowed ($\Delta l=1$) and the $2s$ an optically forbidden transition ($\Delta l=0$) (van den Bos[7]). These selection rules may arise from the relatively large matrix elements $\langle \hat{k}A|r_B^{-1}|\hat{k}'A\rangle$ by expanding r_B^{-1} in spherical harmonics.

Discrete level direct or exchange cross sections to the state k are given from the probabilities via the relation

$$\sigma_k(E)=2\pi\int_0^\infty P_k(b,E)bdb. \tag{59}$$

The ground-state (resonant) charge-transfer cross section is shown in Fig. 7. The curve is monotonically decreasing from 1 keV, with a slight break in slope about 4 keV. The previously obtained curve (WG) indicated a bump at 2 keV which is not present here.

Fig. 8 shows the $2s$ direct and $2s$ exchange cross section curves compared with our previous $2s$ exchange result. The four-state Sturmian calculation is not expected to do as well for $2s$ states as the four-state hydrogenic expansion. The experimental points above 40 keV are due to Ryding *et al.*[8] They lie below these four-state results. (A higher-state point gives better agreement as seen in Sec. VIII.) The $2s$ direct curve (for which no experimental data have been found for comparison) has a broad maximum about 20 keV, while the $2s$ exchange curve exhibits a pronounced peak at the adiabatic 25 keV energy.

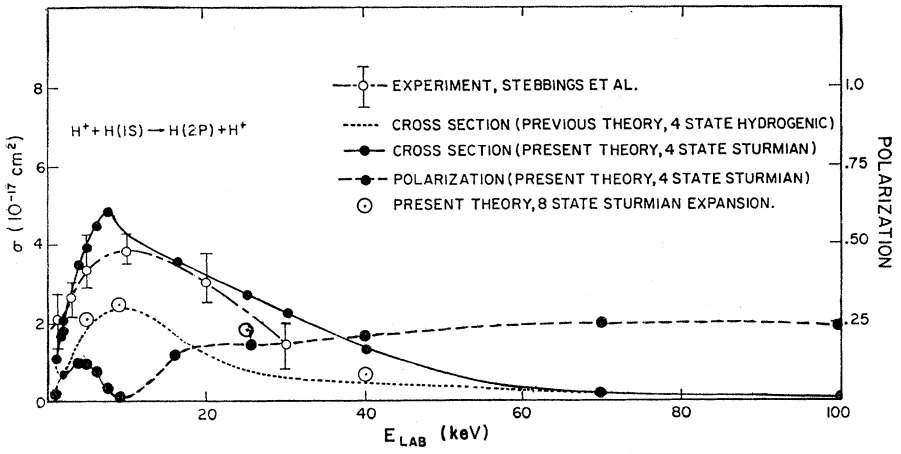

FIG. 9. Cross section and polarization for $2p$ exchange in the four-state expansion. The experimental points of Stebbings *et al.* (Ref. 10) are plotted. The previous four-state ($1s$,$2s$,$2p$,$3s$,$3p$,$4s$) Sturmian calculation. The definition of the polarization is that given by Percival and Seaton (Ref. 9).

[8] G. Ryding, A. B. Wittkower, and H. B. Gilbody, Proc. Phys. Soc. (London) 89, 547 (1966).

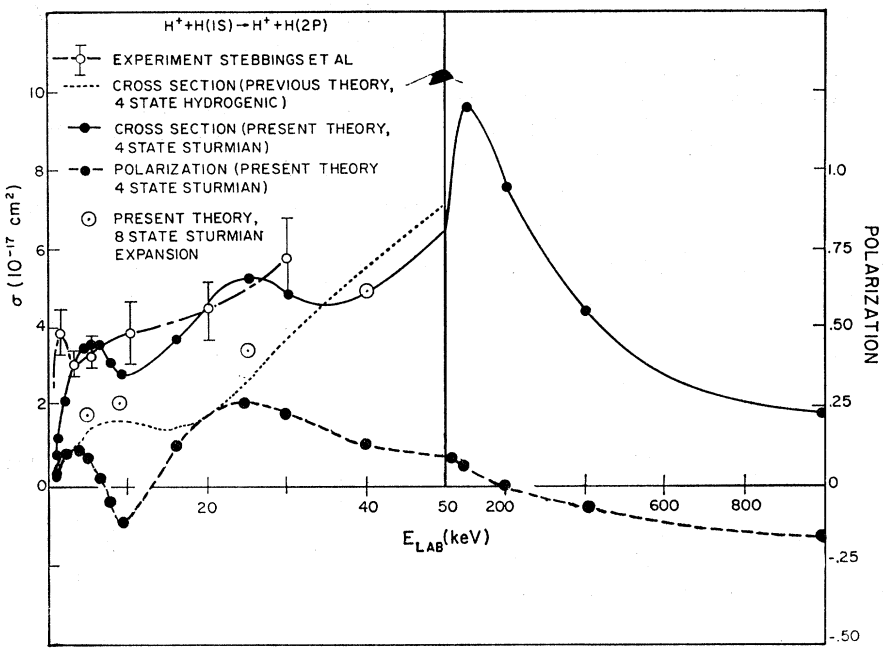

FIG. 10. Cross section and polarization for $2p$ excitation in the four-state expansion. The experimental points of Stebbings *et al.* (Ref. 10) are plotted. The previous four-state hydrogenic curve is plotted and so are circles for an eight-state $(1s,2s,2p,3s,3p,4s)$ Sturmian calculation. The definition of the polarization is that given by Percival and Seaton (Ref. 9).

Figures 9 and 10 give the cross-section and polarization results for $2p$ direct and $2p$ exchange reactions. The polarization fractions have been defined by the formula due to Percival and Seaton.[9]

$$Pol_{np}=\frac{\sigma_{np0}-\sigma_{np\pm1}}{a\sigma_{np0}+b\sigma_{np\pm1}}, \tag{60}$$

with $a=2.375$ and $b=3.749$; this accounts for fine structure and hfs. No experimental data have been found with which to compare the polarization results; however our polarization fractions agree reasonably well at high energies with the asymptotic limits quoted by van den Bos[7] for $2p$ direct (-0.25) and $2p$ exchange (0.27).

Experimental data due to Stebbings *et al.*[10] are plotted on the $2p$ direct and $2p$ exchange curves. Also plotted are the results in WG. The $2p$ direct curve shows two peaks at 6 keV and 25 keV, the magnitudes (but not the shape) of the curve being in good agreement with the data of Stebbings *et al.* The $2p$ exchange curve shows quite remarkable agreement with the results of Stebbings *et al.*, both in magnitude and shape up to about 25 keV, overestimating at energies above 25 keV. Stebbings *et al.*, give error bars at isolated points containing 50% of their data points; they quote their over-all error as $\pm50\%$ and the curve shape error as 15%.

The total-exchange cross section due to McClure[11] is plotted against the theoretical four-state results in Fig. 11. McClure's experimental error is quoted to a $\pm5\%$ accuracy. His last experimental point is at 117 keV. The agreement is excellent up to 25 keV, diverging above 25 keV to a factor-of-2 difference at 40 keV,

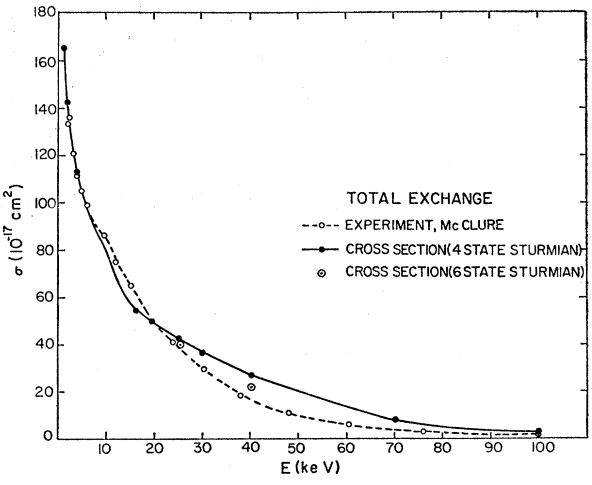

FIG. 11. Total-exchange cross section in the four-state expansion. The experimental data points are due to McClure (Ref. 11). Two points are given for a six-state $(1s,2s,2p,3s,4s)$ Sturmian calculation.

[9] I. C. Percival and M. J. Seaton, Phil. Trans. Roy. Soc. London **251A**, 113 (1959).

[10] R. F. Stebbings, R. A. Young, C. L. Oxley, and H. Ehrhardt, Phys. Rev. **138**, A1312 (1965).

[11] G. W. McClure, Phys. Rev. **140**, A769 (1965).

the theoretical results exceeding the experimental data.

Figure 12 exhibits the data obtained from the experiments of Helbig and Everhart[12] on total exchange probability for 3° scattering compared to our four-state calculations. Not shown are the corrected two-state wave calculations of Francis J. Smith[13] and the three-state ($1s\sigma$, $2p\sigma$, $2p\pi$) molecular eigenfunction expansion calculation of Bates and Williams.[14] Both of these latter results, which are for lower energies (up to about 4 keV), give good agreement with the phase of the oscillating curve, but insufficient damping of the maxima and minima.

We have two four-state calculations; one (the solid line) with b given by the Rutherford elastic scattering formula

$$2Eb=\cot\tfrac{1}{2}\theta, \tag{61}$$

the other (the dotted line) has $b=0$. The agreement of the two curves with data points of Helbig and Everhart is excellent in both magnitude and phase. We believe this to be the best agreement yet obtained with the experiment of Helbig and Everhart.

The point of doing the calculation with $b=0$ is to demonstrate that the total transfer probability is virtually independent of the impact parameter (and hence scattering angle) except for very low energies. This is seen, inasmuch as the dotted and solid curves only begin to separate below 3 keV (see also Helbig and Everhart,[12] Fig. 3).

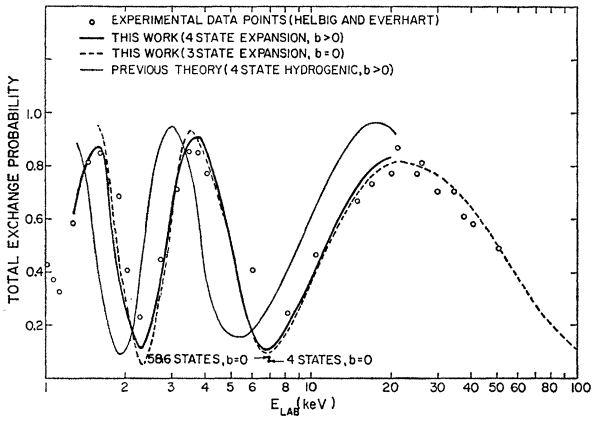

FIG. 12. Total charge-transfer probability at 3°. The experimental data points are due to Helbig and Everhart (Ref. 12). The solid theoretical curve is for the four-state calculation with impact parameter determined from the Rutherford (point) scattering law. The dotted theoretical curve is a three-state calculation for zero impact parameter. Points at 7 keV are for four-, five- and six-state calculations with $b=0$. Not shown are theoretical calculations of Bates and Williams (Ref. 14) (molecular eigenfunction expansion) and Francis J. Smith (Ref. 13) (two-state corrected wave calculation) which yield nearly as good fits below 4 keV.

VIII. HIGHER-STATE RESULTS AND CONCLUSIONS

Having obtained fairly complete results coupling four states ($1s$, $2s$, $2p$) we extended the expansion to include various other states at selected energies and impact parameters. This was to obtain an estimate of the rate of convergence of the expansion. The most definitive sets of calculations are displayed in Fig. 13 for $2p$ processes. As many as nine states are coupled in these calculations. It should be noted that a Sturmian $4s$ state is the same size as a hydrogenic $2p$ state. The inclusion of a $3s$ state was found to be very significant. In general, the convergence of the results is irregular but the trend is toward convergence. The inclusion of a $3d$ state (10 states, not shown) had negligible effect.

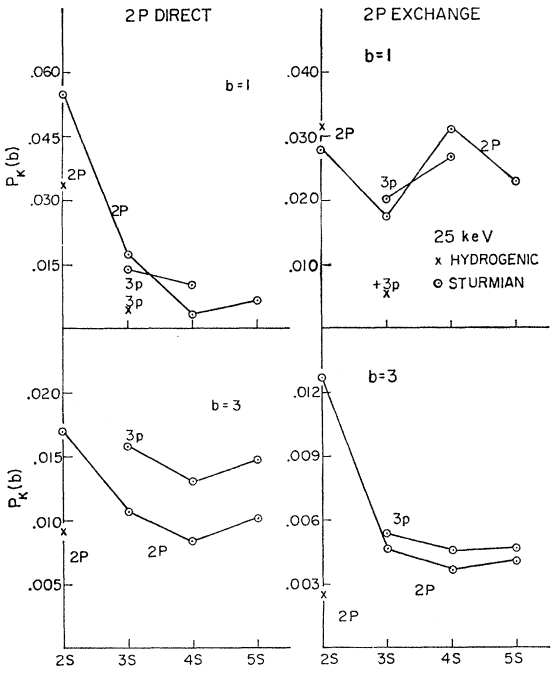

FIG. 13. Dependence of probability on the number of coupled states: $E=25$ keV; $b=1$ and 3; $2p$ direct and $2p$ exchange reactions. The abscissa gives the maximum number of s states included. Points with the same number of p states are connected by line segments. The segments are labelled by the highest p state. The previous results for the hydrogenic expansion are shown for four-state and seven-state calculations. The largest number of states in the calculations is nine.

The impact parameters in this particular study were chosen to accentuate the dependence on the number of states. This is illustrated in Figs. 14 and 15, where $bP(b)$ is plotted against b for the $2p$ processes at 25 keV.

We include the original four-state hydrogenic, the four-state Sturmian, eight-state Sturmian and Born-

[12] H. F. Helbig and E. Everhart, Phys. Rev. **140**, A715 (1965).
[13] Francis J. Smith, Proc. Phys. Soc. (London) **84**, 889 (1964).
[14] D. R. Bates and D. A. Williams, Proc. Phys. Soc. (London) **83**, 425 (1964).

approximation results (van den Bos[7]) plus an isolated nine-state point. Noteworthy is the asymptotic agreement at large b among all curves, the only discrepancy here being the $2p$ exchange Born curve of van den Bos,

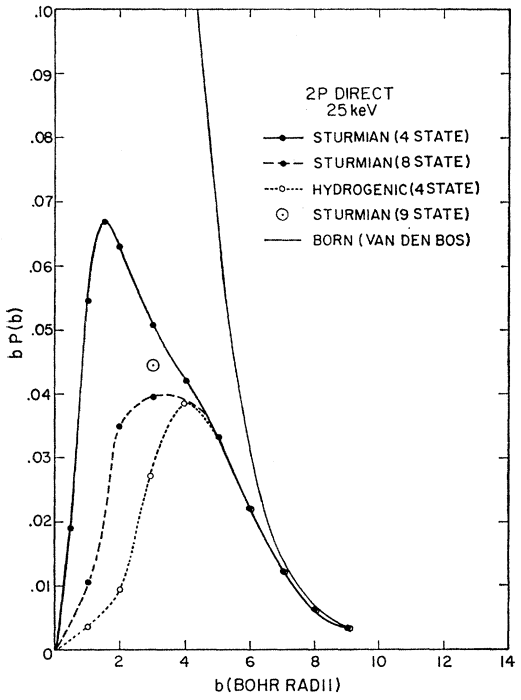

FIG. 14. Probability times impact parameter versus impact parameter for $2p$ excitation at 25 keV. Shown are four-state and eight-state Sturmian curves, the previous hydrogenic four-state curve, and a single Sturmian nine-state $(1s,2s,2p,3s,3p,4s,5s)$ point.

which does not agree with the other results. This is not completely understood, but may be due to the quite different manner of calculation which van den Bos used for his exchange than for his direct Born approxi-

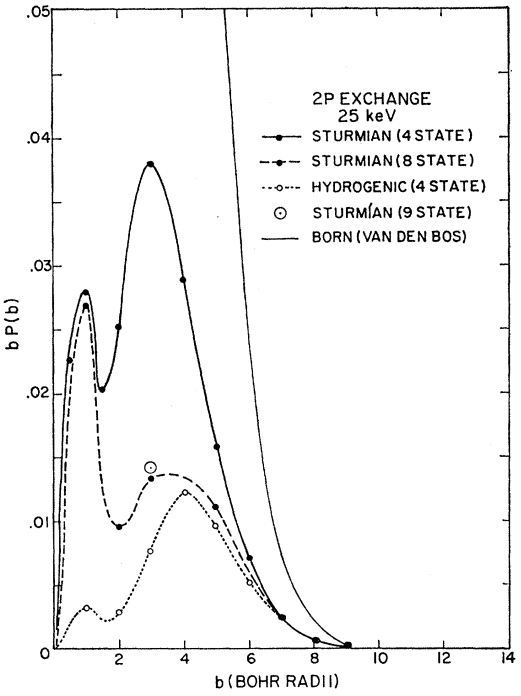

FIG. 15. Probability times impact parameter versus impact parameter for $2p$ exchange at 25 keV. Shown are four-state and eight-state Sturmian curves, the previous hydrogenic four-state curve, and a single Sturmian nine-state $(1s,2s,2p,3s,3p,4s,5s)$ point.

mations. The asymptotic agreement for direct excitation, however, may permit one to omit the complex coupled equations method for large b, using Born results there.

A careful examination of Figs. 13–15 lends confidence to the eight-state calculation for $2p$ processes. We believe that such results are reliable to 20%, and perhaps considerably better. Eight-state results are presented in Figs. 9 and 10 at selected energies (as obtained from a relatively small number of impact parameters). The results are systematically lower than the experimental results of Stebbing *et al.*